Larger air lines in heavy vehicle suspensions – differences in wheel and air spring forces

Lloyd Davis[1,2] and Jonathan Bunker[1]

[1] Queensland University of Technology
[2] Queensland Department of Main Roads

1   Introduction

The Australian transport industry is focused heavily on road transport. Additional payload is allowed by most road authorities for heavy vehicles (HVs) equipped with "road friendly" suspension (RFS). The move to higher payloads using HVs with RFS has allowed the road freight industry to absorb some of the increasing demand for long-haul freight.

The first RFS were air-sprung and most still are, although some steel-suspended RFS are coming on to the market (DOTARS, 2004a). Davis and Sack (2004) indicated that dynamic load sharing (*i.e.* transfer of air within the group) was not a feature of conventional HV air suspensions. This was noted for the case particularly between consecutive axles, since air suspensions with industry-standard small-diameter longitudinal air lines did not allow the quick movement of air between air springs on sequential axles. Previous research has documented reductions in dynamic axle-to-chassis forces (Davis, 2006a) as well as reductions in dynamic wheel forces (Davis, 2007) by increasing the size of longitudinal air lines on air sprung HVs. That work also showed that the installation of larger longitudinal air lines increased load equalisation between axles.

This paper provides more extensive results than previously published of a test regime to explore whether longitudinal air line size affects dynamic forces in HV air suspensions. The treatment test case was for a proprietary suspension system, where larger longitudinal air lines connected the test vehicles' air springs. Figure 1 (left) shows this system schematically. Transverse air lines were not altered, as required by the manufacturer of the system tested. Note that some detail has been removed from this figure for clarity. Larger air lines run longitudinally and connect air springs fore-and-aft.
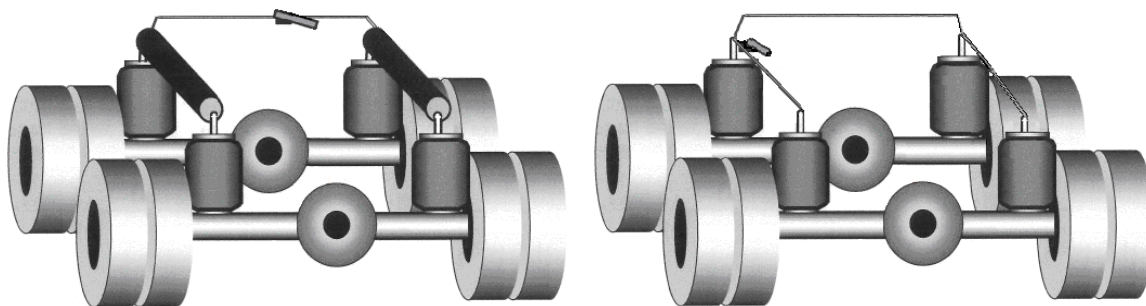
Figure 1 – Schematic layouts of "Haire" (left) and standard (right) air suspension systems

The tests comprised driving three HVs at a variety of speeds over a series of typical, uneven road sections. For both cases of standard longitudinal air lines (initial) and larger longitudinal air lines (treatment), dynamic forces were recorded at the air springs and the pavement. Dynamic measures such as the dynamic load coefficient (DLC), load sharing coefficient (LSC), peak dynamic suspension force (PDSF), dynamic impact factor (DIF) and dynamic load sharing coefficient (DLSC) were derived from the axle-to-chassis forces, with and without larger longitudinal air lines.

Further, the DLC, LSC, DLSC, DIF, road stress factor (RSF) and peak dynamic wheel force (PDWF) were derived for wheel/pavement forces for the initial and treatment cases.

The aim of this paper is to detail further analysis from the test programme to that already published (Davis, 2007). The results lead to conclusions regarding the probability that HV dynamic wheel load forces being transmitted to pavements and within the vehicle at the chassis/spring interface may be reduced by fitting larger longitudinal air lines, thus saving on road and vehicle damage and pavement rehabilitation costs.

2   Background

The inability of HVs with air suspension to equalise load between sequential axles was noted in the final report of the DIVINE project (OECD, 1998). That report also noted (p77) that air-sprung HVs induced up to 4.5 times the dynamic load allowance specified in bridge design because of the "very limited dynamic load sharing" of air suspensions. The DIVINE project report (p107) stipulated that suspension load equalisation was important to "road-friendliness" but ultimately recommended a load equalisation metric that did not include any dynamic component (OECD, 1998). The Australian VSB 11 RFS specification requires compliant suspensions to have static load sharing (DOTARS, 2004b). That document does not address dynamic load sharing. Further, neither it nor any other official document defines a formal methodology to determine static load sharing for a HV (Prem *et al.*, 2006).

One definition of dynamic load sharing is "dynamic equalisation of axle group loads across all wheels/axles at typical vehicle operating conditions". Various efforts have been made to develop a measure for this concept, such as the LSC and the DLC (Sweatman, 1983). Clarification of a methodology and definition of load sharing occurred subsequently (Potter *et al.*, 1994, 1996; Mitchell and Gyenes, 1989; Gyenes and Mitchell, 1994; Fletcher *et al.*, 2002). Despite these efforts, there is still no agreed testing procedure to define or measure dynamic load sharing at the local or national level in Australia.

Estill *et al.* (Estill and Associates Pty Ltd, 2000) and Roaduser (Roaduser Systems Pty Ltd, 2002) reported anecdotal evidence of the successful use of larger diameter air lines on air-sprung HVs. This has not been confined to the "Haire system" (Davis, 2006a; Willox, 2005) and has been implemented as original equipment on Kenworth/Paccar HVs, for example.

3   Experimental procedure

Previous papers documenting this research programme have examined alterations to dynamic forces between the axle and the chassis (Davis, 2006a) and on wheel forces (Davis, 2007) from fitting larger longitudinal air lines. This paper examines in more detail the results of this research programme. The testing procedure used for that work and this paper has been provided previously (Davis, 2006a, 2007; Davis and Bunker, 2008) but is reiterated here briefly for context.

Three HVs were used for the testing: a tri-axle semi-trailer towed with a prime mover, an interstate coach with three axles, and a school bus with two axles. Instrumentation consisted of strain gauges, accelerometers, and air pressure transducers (APTs). These were installed on the tri-axle group of the semi-trailer, the drive and tag axle of the coach and the drive axle of the school bus. The air springs of the axles/axle group of interest were configured such that they could be connected using either standard air lines or larger-than-standard longitudinal air lines. The drive axle of the coach and the drive axle of the school bus had a four-spring configuration supporting the chassis at that axle. These axles had longitudinal beams attached slightly inboard of the hub on either side, and an air spring on each end of

the beams (Figure 5). The tag axle on the coach had an air spring mounted above it on either end. Figure 2 to Figure 10 show photos, diagrams and details of the test vehicles.

The drive axle of the school bus had no corresponding axle with which to "share" its air transfer. Accordingly, the modification to the bus was that larger air lines were connected to the front and rear air springs on either side of the drive axle (Figure 5). Whilst the effect of air transfer on forces between wheels on one axle was not within the scope of this paper, alterations in dynamic forces due to "front-to-back" air transfer for this bus' air springs during the tests was analysed.

Figure 2 – Prime mover (left) used to tow the test trailer (right)

Note: The prime mover's suspension was not tested in this series.

Figure 3 – 3-axle coach used for testing

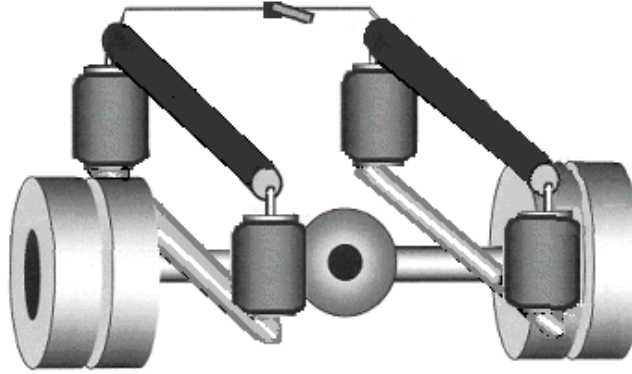**Figure 4 – 2-axle school bus used for testing (left) and yellow sacks of horse feed used to load bus and coach (right)**

Figure 5 – Schematic layout of the larger longitudinal air lines as implemented for drive axle on 2-axle school bus

Figure 6 – Large longitudinal air line used in the "Haire suspension system"

3.1   Equipment and instrumentation

At the hubs of the wheel/s of interest, strain gauges were mounted on the axle's neutral axis (Woodroofe *et al.*, 1986; de Pont, 1997) to measure static wheel loads and dynamic wheel loads (less the inertial component of dynamic wheel forces due to the mass outboard of the strain gauges). Figure 7 top left and top right shows examples of these under waterproofing foil, and Figure 7 bottom right shows them exposed. Mounting on the neutral axis ensured that bending moments imparted to the axles by lateral forces on the wheels were not measured by the strain gauges. This provided less complex sets of data that were more easily analysed because they did not include lateral wheel forces (de Pont, 1997). The strain gauges were calibrated *per* Woodrooffe *et al.* (1986) for each wheel of interest.

Accelerometers were mounted at each hub of the wheel of interest to measure vertical acceleration of the axle/hub/wheel mass outboard of the strain gauges. Figure 7 top right shows the tag axle arrangement (yellow bracket) for the accelerometer. Figure 7 top left (yellow bracket) and Figure 8 show typical arrangements for accelerometer mounting plates fixed to the axles. Dynamic wheel forces produced by the inertial effect of the mass of the axle and other attached masses (for example, brakes, wheels, hubs, etc) outboard of the strain gauges were derived by combining the data from the accelerometers and the strain gauges (de Pont, 1997) *per* Equation 1 below.

Air pressure transducers (APTs) were mounted in the air lines to the air springs as shown in Figure 9. They were used to measure the air pressure in each air spring and therefore the static and dynamic forces between the axle at that spring and the chassis.

Daily checks on the quiescent outputs of the instruments showed slight variations due to vehicle supply voltage fluctuations. The steady-state values were noted and the relevant calculations or calibration graphs adjusted accordingly.

An advanced version of the TRAMANCO on-board CHEK-WAY® telemetry system was used to measure and record the dynamic signals from the outputs of the strain gauges and accelerometers. Figure 10 shows the CHEK-WAY® recording system used for the tests.
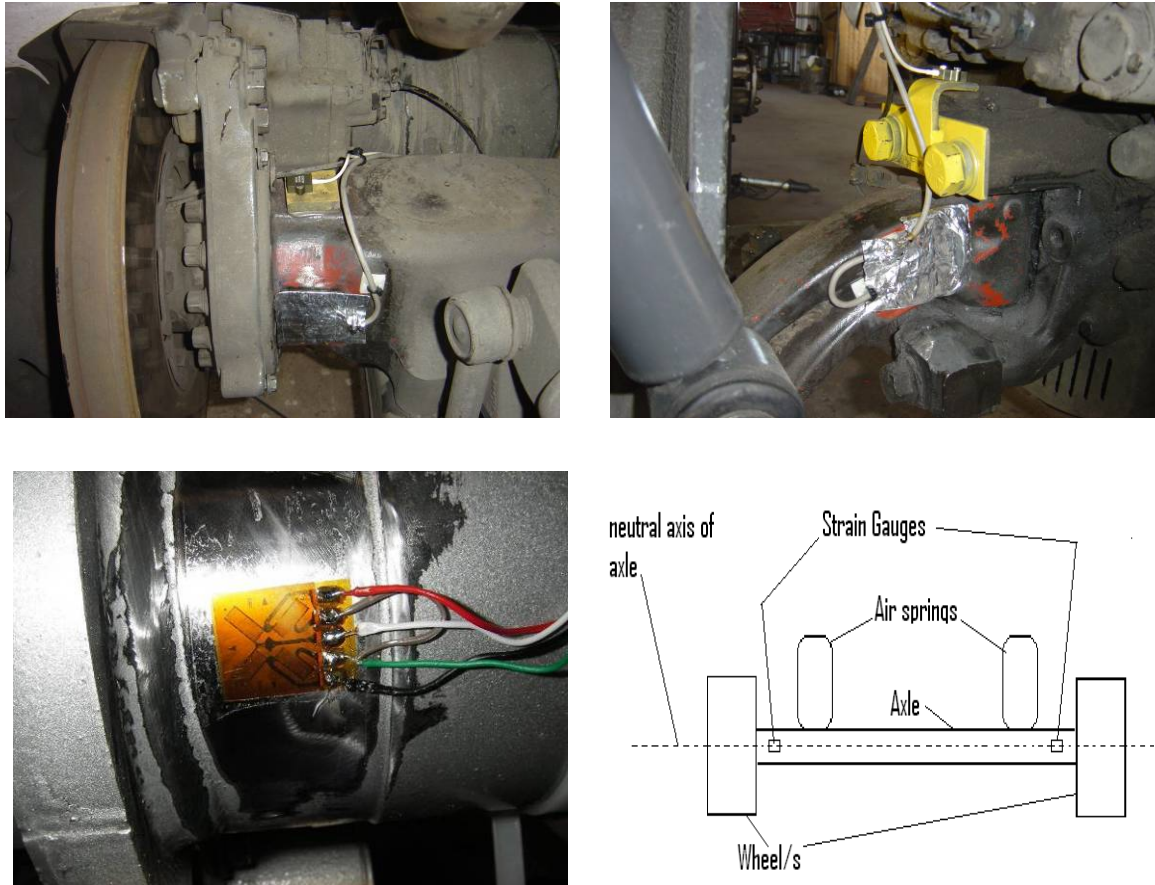
Figure 7 – Accelerometer and strain gauge mounting (under waterproofing foil) for drive axle of coach (top left) and for tag axle of coach (top right). Semi-trailer axle strain gauge (bottom left) and schematic of strain gauge layout (bottom right).
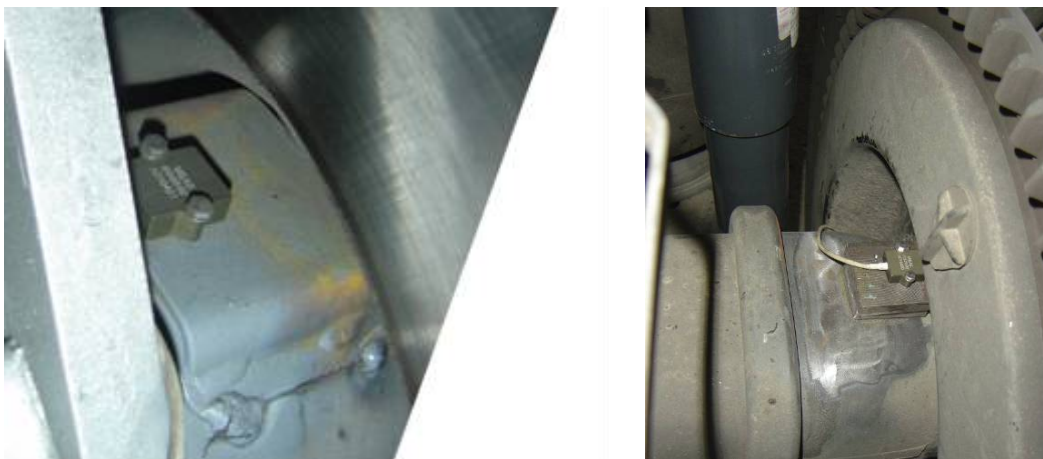
Figure 8 – Accelerometer mounted on top of trailer axle (left) and school bus (right)
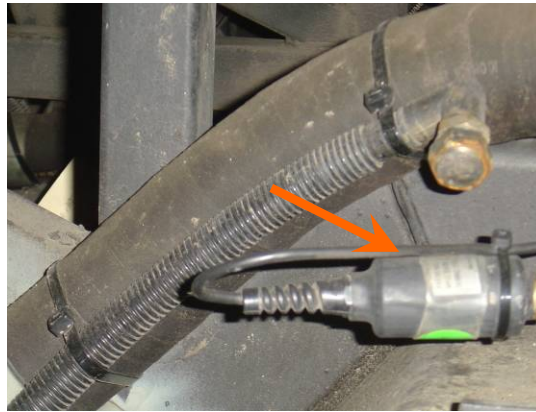
Figure 9 – Typical air pressure transducer (arrowed) used for measuring forces at air springs

Figure 10 – Data capture management computers (left) and data capture and storage telemetry units (right) installed on a bus

The telemetry system sampling rate was 1 kHz, giving a sample interval of 1 millisecond. Note that the natural frequency of a typical heavy vehicle axle is 10 to 15 Hz (Cebon, 1999) compared with a relatively low frequency of 1 to 3 Hz for the sprung mass (de Pont, 1999). Any attempt to measure relatively higher frequencies (such as axle-hop) using time-based recording will necessarily involve a greater sampling rate than when relatively lower frequencies (such as the body-bounce frequency) are to be determined (Houpis and Lamont, 1985). Axle-hop was the highest frequency of interest for the analysis undertaken. The 1 kHz sampling frequency used exceeded the minimum required to capture the test signal data since its sample rate was much higher than twice any axle-hop frequency. The Nyquist criterion (Shannon's theorem) for the sampling frequency to be at least twice that of the signal of interest frequency (Houpis and Lamont, 1985) was more than satisfied by using this approach.

3.2   Procedural detail

The HVs were driven over a series of typical, uneven road sections for the initial test case of standard longitudinal air lines in two load conditions (tare and loaded) and for speeds from 40 km/h to 90 km/h. For the treatment test case, the standard longitudinal air lines between the air springs were disconnected and the larger longitudinal air lines between the air springs installed. The HVs were then driven over the same road sections using the same wheel-paths at the same speeds as the previous tests at tare and full load. At least two runs for each speed were made. Some 60 km/h sections were traversed up to 5 times.

Figure 13 illustrates, by example, the adherence to wheel-paths followed by the driver during the testing. We see the road unevenness, as stimulus events, occurring at almost identical times relative to the recording start for each signal. The data from each APT, accelerometer, and strain gauge were recorded at 1 kHz resulting in a test data set in the form of a 10 s time-series signal from each APT, each accelerometer and each strain gauge from each axle-end of interest. This data set was for each test HV, for the initial and treatment test cases, at the various test speeds and the two loading conditions.

4   Analysis

The instrumentation described above allowed determination of dynamic wheel forces. Dynamic wheel force can be expressed by the formula (Woodroofe *et al.*, 1986):

$$F_{wheel} = F_{shear} + ma$$ Equation 1

F_{shear} was measured from the strain gauges on each axle-end after calibration. The value of *m*, representing the axle/hub/wheel masses outboard of the strain gauges, was determined by various means such as manufacturer's data, weighing wheels on certified scales, or cutting through an axle at the strain gauge mounting point and weighing the axle remnant (Figure 11 and Figure 12). The measured mass (comprising the mass outboard of the strain gauges) was multiplied by the dynamic acceleration value, *a*, and this product added to the instantaneous F_{shear} to derive dynamic F_{wheel} for each wheel (de Pont, 1999).

Using the dynamic F_{wheel} data, DLSC, LSC, PDWF, DLC, DIF and RSF were derived to determine alterations to dynamic wheel-forces, if any, due to the fitment of the larger longitudinal air lines in the treatment test case. Analysis of the statistical significance of any alterations to these measures is shown in the results, Section 5. The bus DLSC was not derived since this HV did not have a sequential axle with which to "share" the load from the drive axle. Similarly, with the exception of deriving the bus drive axle LSC for error analysis purposes (Section 5.1) the bus drive axle LSC was not analysed for statistical significance since the transverse air line was not altered for these tests.

Figure 11 – Weighing the half-shaft mass outboard of strain gauges (left) and mass of bus drive axles outboard of strain gauges (right)

Figure 12 – Weighing the axle mass outboard of the strain gauges for the tag axle (left) and the drive axle (right)
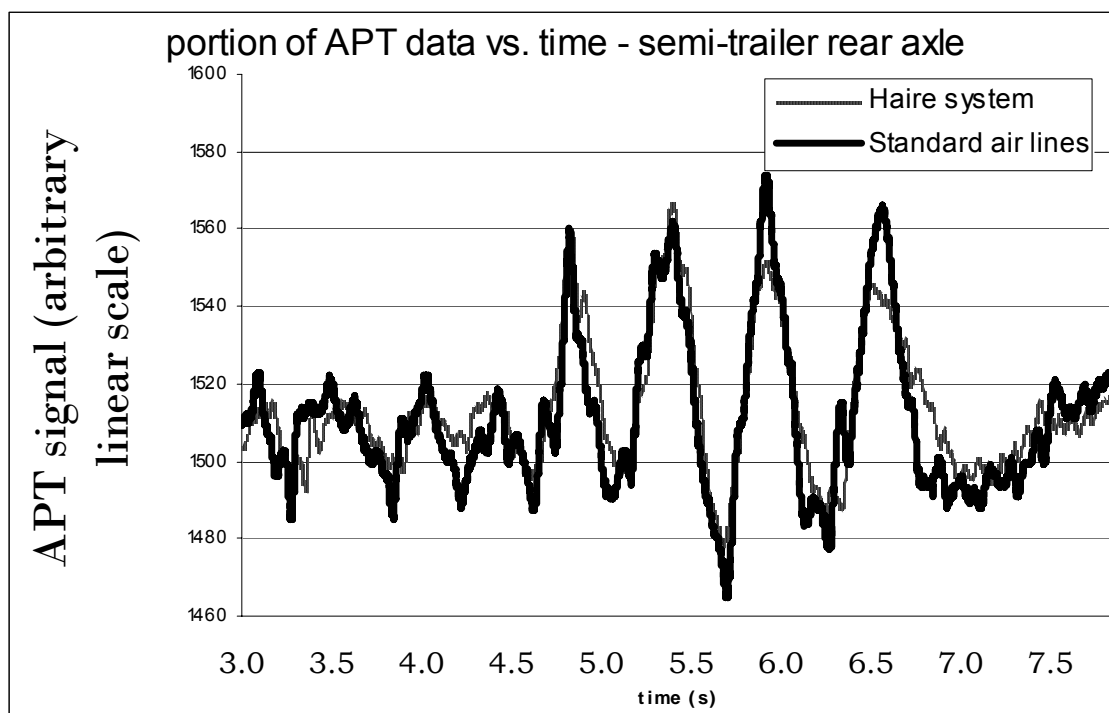

Figure 13 – Example of test traces showing difference in signals for initial case of standard longitudinal air lines (solid line) and for treatment case of fitment of "Haire system" (dotted line) over the same road section

Figure 13 is a plot of a portion of two traces of wheel-force data for one wheel. It shows the difference in the magnitude of the measured signals (dynamic wheel forces) at the wheels of the HV under test, between the initial standard-sized longitudinal air lines and the treatment (Haire suspension system) case. It also shows typical measured wheel force data.

The LSC, DLC, DIF, DLSC, and peak dynamic suspension force (PDSF) at the chassis-to-axle interface were derived by substituting APT data for wheel load data in equation 1 above.

5   Results

Table 1 and 2 summarise statistical analysis using a t-test to determine the significance of positive changes to the various dynamic measures, for the initial (standard air lines) and treatment (larger air lines) cases respectively. A heteroscedastic test option was chosen since the data from the two test cases had unequal variances (Kariya and Kurata, 2004) over the range of test speeds. A one-tailed test was used since a) previous work (Davis, 2007) and the background analysis (to be published in future) on the dynamic measures from the APTs indicated that the larger longitudinal air lines generally improved dynamic measures (StatPac Inc, 2007) and b) the other tail would inform the case where performance was improved beyond the confidence limit (Hamburg, 1983). A value for α = 0.1 was chosen since road-damage or HV improvements are judged *via* business cases which use this α value as an upper bound. This choice of α is conservative; 0.2 has been used for business cases in mechanical engineering applications with skewed distribution data (Kleyner, 2005). A green cell in either table indicates that $\alpha \leq 0.1$, or that there is a less than 10% chance that any positive alteration to that particular dynamic measure was by chance; that is, a 90% confidence value that the larger longitudinal air lines altered the mean of the dynamic data in a positive manner for the corresponding speed.

Alterations to some wheel-force measures for larger longitudinal air lines have been provided in previous papers, notably Davis (2007). Future papers will provide the quantum of those changes as well as changes to axle-to-chassis forces when larger longitudinal air lines were fitted. These have been held over due to space limitations.

A dynamic measure, the DLSC (de Pont, 1997) not previously derived and published for these data, is included here for wheel and axle-to-chassis forces. Since the alteration to the suspensions was for longitudinal air lines, any alteration to transverse load sharing can be neglected since this was not altered. Accordingly, the DLSC for each side of the coach and the semi-trailer was derived.

5.1   Error analysis

Dynamic and inertial forces at the wheels vary constantly. A conclusive overall error valid for all conditions cannot be derived, therefore (Cole, 1990). Previous estimates of wheel-force error in dynamic measures have varied from 3% to 6.6% (Cole, 1990; Mitchell and Gyenes, 1989). These studies considered dynamic measures and used aggregated data to derive DLC (for instance Cole, 1990).

The test programme detailed in this paper instrumented the mass outboard the strain gauges with accelerometers. The readings from these, combined with strain gauge data, were used to derive both static and dynamic wheel-forces. This method used modern instrumentation to reduce the errors for our test programme as shown below. Dynamic measures using instantaneous data points such as DLSC also assisted in reducing error. It is for noting that Cole (1990) documented an error of 6.6% because that study did not measure or record the mass nor derive dynamic inertia outboard of the strain gauges. The contribution of these to the overall dynamic wheel-forces was simply estimated for that work (Cole, 1990).

Overall errors in the wheel force measurements were due to the errors in the accelerometer and strain gauge readings. Errors in the air-spring measurements were due to the accumulated errors in the chain from the APTs to the telemetry outputs. The telemetry system recorded over a 10 second period at 1.0 kHz, yielding ten thousand values for every transducer during each test. Figure 14 shows LSC *vs.* Speed for the bus at full load.

A cross-check for overall error may be made as:

- The LSC uses an average of instantaneous wheel force and divides it by the wheel force of the group; but

- the bus had only 2 wheels under test, therefore:

- the LSC averaged *per* test speed for the bus should equal 1.0.

Any deviation from 1.0 for the bus LSC was therefore due to a combined measurement error at the strain gauges and the accelerometers. It was a maximum of 1.5% at 90 km/h. LSC was derived by averaging ten thousand values across all transducers. We see that this was indicative of the wheel-force error *per* axle for all the dynamic measures that used such averaging (*e.g.* LSC and DLC). If using ten thousand values resulted in an accumulated error of 1.5%, the error *per* instantaneous value was therefore small. DLSC, PDWF and DIF were derived from instantaneous values of wheel-force, not data points aggregated as for LSC and DLC. The errors in deriving DLSC, PDWF and DIF were much smaller than 1.5%.

Overall error of APTs and the telemetry system used for these tests has been documented previously at ±1.0% (Davis, 2006b). A 2% inaccuracy for air-pressure transducer measurement has been reported elsewhere (Transport Certification Australia, 2007).

Overall error of strain gauges feeding the telemetry system used for these tests can be seen in examples provided in Figure 15 and Figure 16. These graphs have been documented in full elsewhere (Davis and Bunker, 2008) but extracts have been provided here by way of example. The regression line R^2 values varied from 99.22% (worst) for one strain gauge on the coach to 100% (best) for the semi-trailer (Davis and Bunker, 2008). These indicated that the errors in strain gauge readings were, at worst, very small.

As noted above, the data from the runs for the two test cases had unequal variances for each test speed; that is, the dynamic measures were not Gaussian per test speed. Accordingly, standard deviations of derived dynamic measures became meaningless and required a heteroscedastic test option (Kariya and Kurata, 2004).
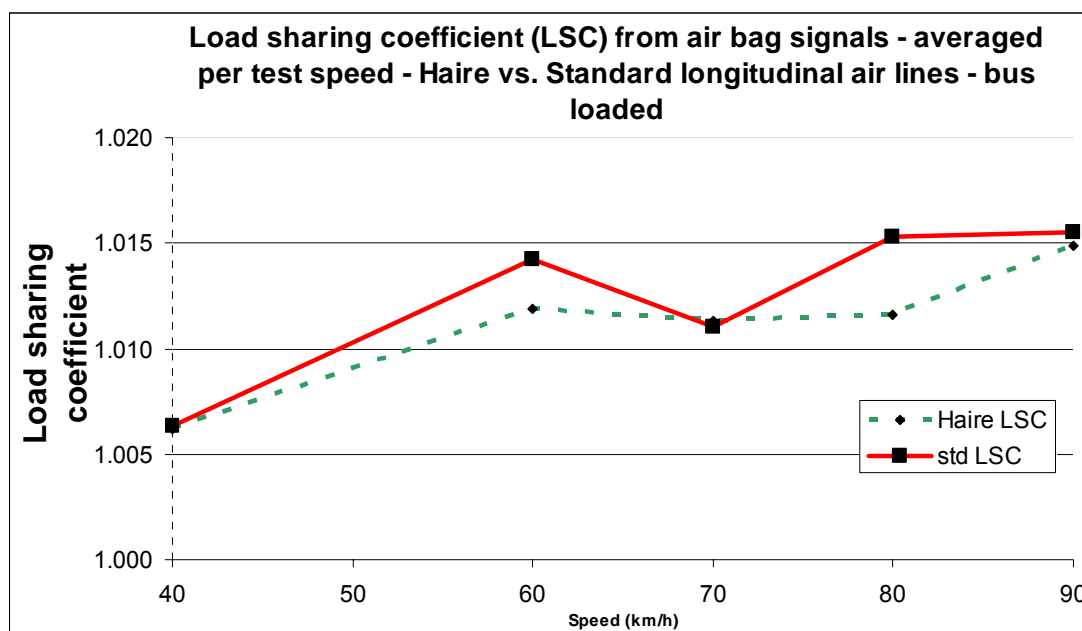

Figure 14 – Load-sharing coefficient for the air springs on the bus at full load averaged at each test speed
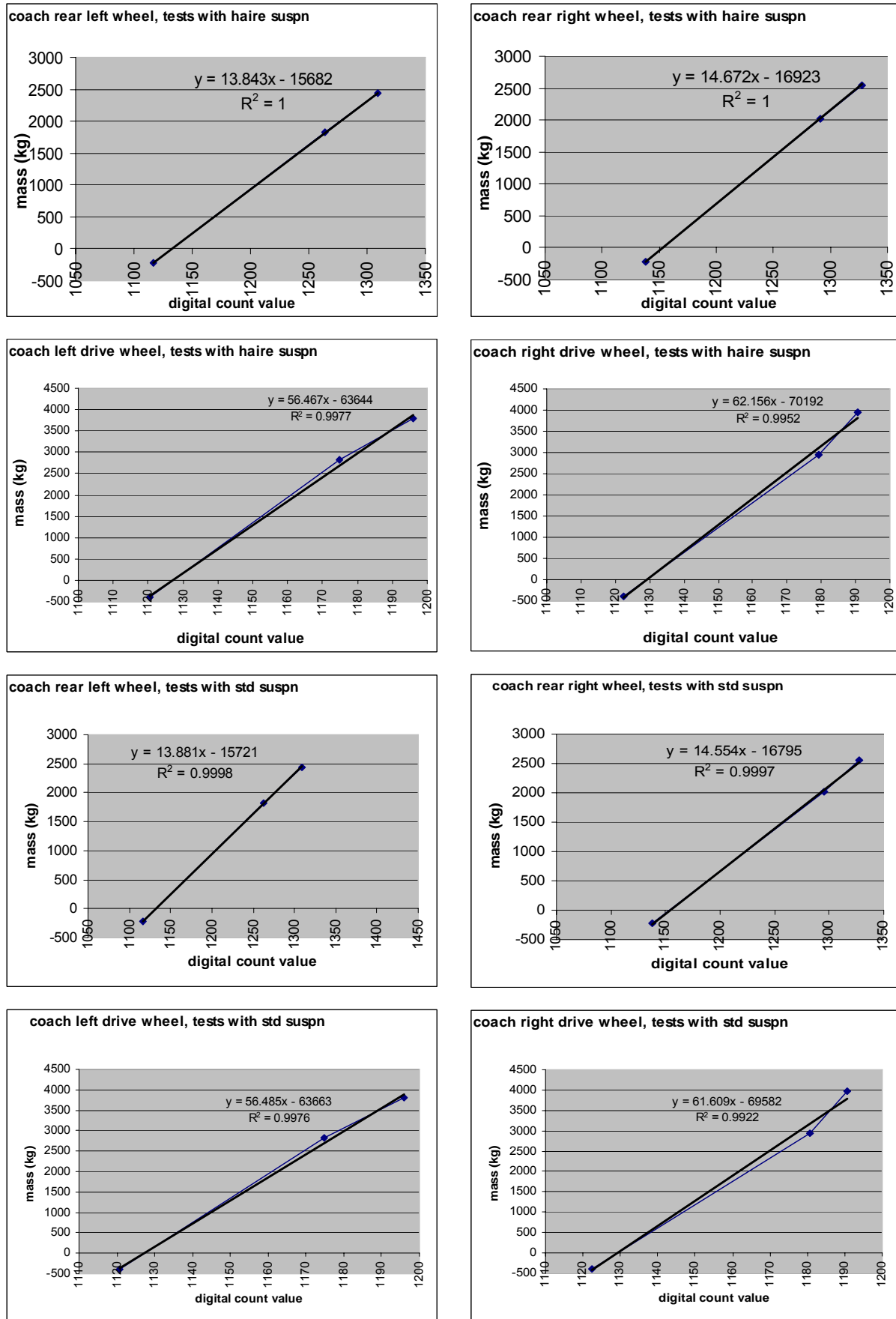
coach rear left wheel, tests with haire suspn

$y = 13.843x - 15682$
$R^2 = 1$

coach rear right wheel, tests with haire suspn

$y = 14.672x - 16923$
$R^2 = 1$

coach left drive wheel, tests with haire suspn

$y = 56.467x - 63644$
$R^2 = 0.9977$

coach right drive wheel, tests with haire suspn

$y = 62.156x - 70192$
$R^2 = 0.9952$

coach rear left wheel, tests with std suspn

$y = 13.881x - 15721$
$R^2 = 0.9998$

coach rear right wheel, tests with std suspn

$y = 14.554x - 16795$
$R^2 = 0.9997$

coach left drive wheel, tests with std suspn

$y = 56.485x - 63663$
$R^2 = 0.9976$

coach right drive wheel, tests with std suspn

$y = 61.609x - 69582$
$R^2 = 0.9922$

Figure 15 – Examples of the calibration of the strain gauges on the coach
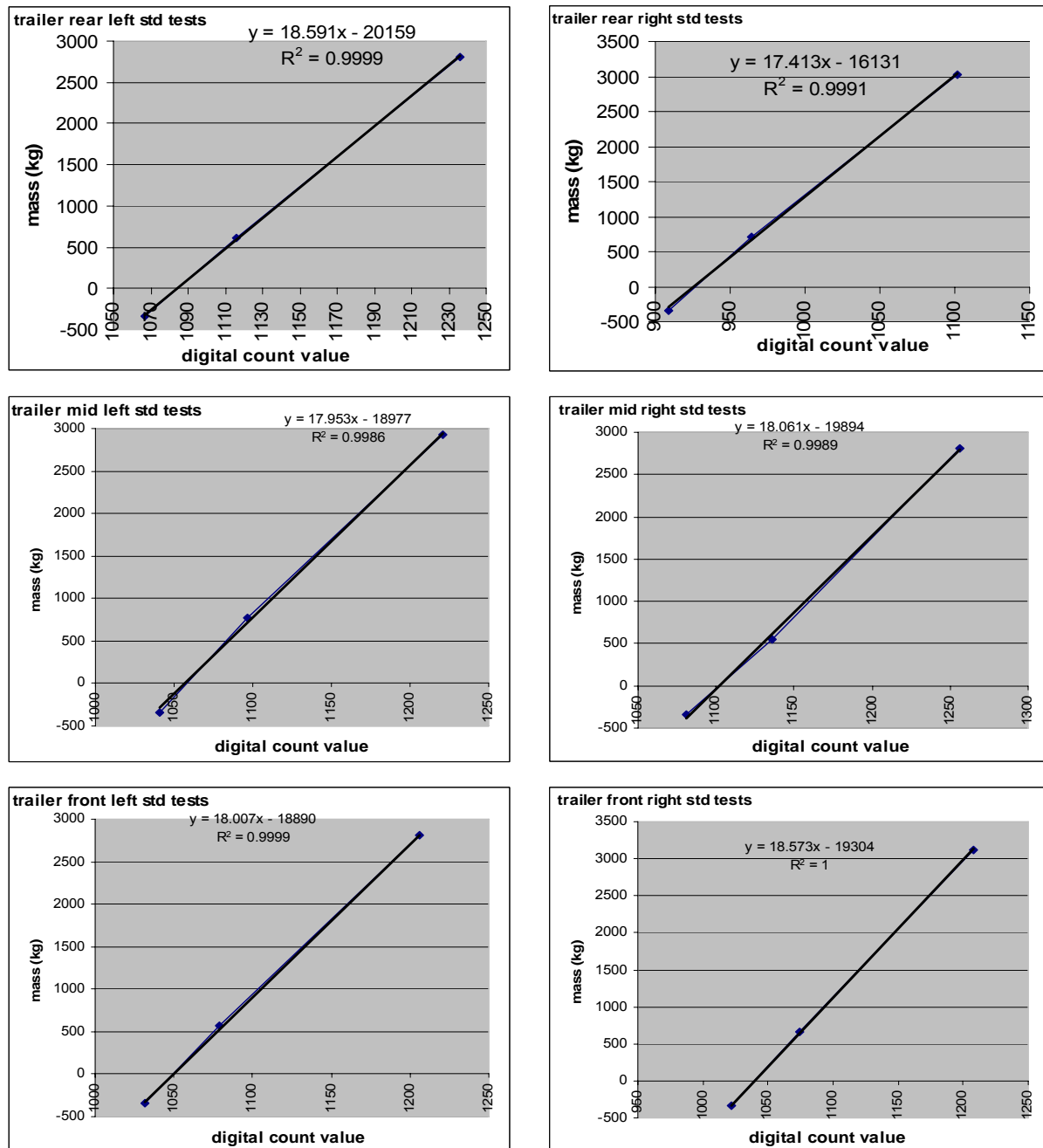
Figure 16 – Examples of the calibration of the strain gauges on the semi-trailer

6   Discussion

Table 1 and 2 show where larger longitudinal air lines have altered the dynamic measures for the test vehicles positively, by a statistically significant amount. In addition to the standard measures for suspension dynamic parameters, this study applied an innovative measure to the multi-axle vehicles. This was the Dynamic Load Sharing Coefficient (DLSC) applied *per side* to the coach and the semi-trailer. The results for each side's DLSC indicate that front-to-back load sharing was improved at the air springs in the semi-trailer when larger longitudinal suspension air lines were used, for every test speed and load, except tare at 80 and 90km/h. Similar improvements may be seen at lower speeds for the loaded coach. Also notable is the uniform alteration to the PDSF for the bus at all speeds. Whilst this test vehicle had no other axle with which to "share" its drive axle dynamic loads, the results in

Table 1 suggest that, as previously hypothesised (Davis, 2007), the larger air lines were acting as accumulators to reduce axle-to-chassis dynamic forces. This effect has now been shown to be statistically significant.

Previous work on the vehicles tested as described herein (Davis, 2007) and other test vehicles with larger longitudinal air lines fitted (Davis, 2006a) has shown that no dynamic performance parameter was adversely affected by their fitment. For these tests, by considering the dynamic measures, most of the improvements were at the axle-to-chassis interface (the air springs) rather than for wheel-force. The proposal that dynamic factors have been enhanced positively should alert HV manufacturers to the possibility of savings or economies in this area of HV design. It also goes some way toward explaining both the anecdotal (Roaduser Systems Pty Ltd, 2002; Estill and Associates Pty Ltd, 2000) and documented (Willox, 2005) evidence from transport industry stakeholders regarding the benefits in fitting larger longitudinal air lines. This is particularly for those alterations noted in the ride, the predominant control of which is by axle-to-chassis interaction.

More analysis needs to be performed to explain the reasons for the disparity from one dynamic measure to another; this will be the subject of future papers. Nonetheless, as pointed out by various researchers (de Pont, 1997; Cebon, 1999; Potter *et al.*, 1996), no single dynamic measure has yet been developed to define quantitatively what constitutes a "good" HV suspension or one which produces the least pavement damage. It is noted that dynamic measures such as the DLC (and, by inference, the RSF which is derived from the DLC) have been criticised by Cebon (Lundström, 2007). These measures yield a result after aggregation of instantaneous data. Dynamic measures developed more recently are exemplified by the DLSC, the DIF and the PDWF. These are metrics derived from instantaneous data points found without aggregation or less aggregation than the more traditional measures such as the DLC.

De Pont (1997) criticised the LSC as merely a measure of average load sharing behaviour since it is found by averaging load sharing over a test run or length of tested road. However, this observation and further consideration of the DLSC measure itself needs to be researched further, with the potential for the DSLC to be used more widely.

7   Conclusion

The results of this study showed that the treatment case of larger longitudinal air lines on air sprung heavy vehicles altered dynamic forces. This led to improvements in dynamic forces at the springs and wheels to a 90% confidence value. The improvements were non-uniform and more in evidence at the springs than at the wheels. Implementing the treatment case and thereby reducing the forces at the body-to-chassis interface should lead to savings or economies in HV chassis design. This should logically lead to lighter chassis and therefore increased payloads for the same gross vehicle mass. It would be expected that the HV manufacturing industry would research and make wider use of the design feature tested herein, as has been done by a limited number of manufacturers (such as Kenworth/Paccar) and as noted in other specialised applications (Estill and Associates Pty Ltd, 2000; Roaduser Systems Pty Ltd, 2002).

Table 1 – T-test analysis of axle-to-chassis dynamic measures altered positively by the fitment of larger longitudinal air lines.

█ **indicates a statistically significant alteration to a 90% confidence interval.**

Speed (km/h)	Vehicle	Measures Derived From Axle-To-Body Forces						
	Trailer	DLC	LSC	DLSC	DIF	PDSF	DLSC LEFT	DLSC RIGHT
40	loaded	█	█	█	█	█	█	█
60				█			█	█
80							█	█
90							█	█
40	tare	█	█	█			█	█
60		█		█			█	█
80								
90								

Speed (km/h)	Coach	Tag DLC	Drive DLC	Tag LSC	Drive LSC	Tag DLSC	Drive DLSC	DLSC LEFT	DLSC RIGHT	Tag DIF	Drive DIF	Tag PDSF	Drive PDSF
40	loaded						█	█		█	█		
60			█	█			█	█	█	█	█	█	█
80			█	█									
90			█		█	█						█	
40	tare			█		█		█	█				
60													
80				█									
90													

Speed (km/h)	Bus	DLC	DIF	PDSF
40	loaded		█	█
60				
80			█	█
90			█	█
40	tare		█	█
60			█	█
80			█	█
90				█

DLC: Dynamic load coefficient; LSC: Load sharing coefficient; DLSC: Dynamic load sharing coefficient; PDSF: Peak dynamic suspension force; DIF: Dynamic impact factor.

Table 2 – T-test analysis of wheel-force dynamic measures altered positively by the fitment of larger longitudinal air lines.

▓▓▓▓ **indicates a statistically significant alteration to a 90% confidence interval.**

Trailer

Speed km/h	Trailer	DLC	LSC	DLSC LEFT	DLSC RIGHT	DLSC	DIF	PDWF	RSF
40	loaded		▓	▓	▓				
60									
80			▓						
90									
40	tare								
60			▓						
80									
90									

Coach

Speed km/h	Coach	Tag DLC	Drive DLC	Tag LSC	Drive LSC	Tag DLSC	Drive DLSC	DLSC LEFT	DLSC RIGHT	Tag DIF	Drive DIF	Tag PDWF	Drive PDWF	Tag RSF	Drive RSF
40	loaded			▓						▓	▓				
60					▓					▓		▓			
80															
90				▓											
40	tare			▓											
60															
80															
90															
80			▓												
90															

Bus

Speed km/h	Bus	DLC	DIF	PDWF	RSF
40	loaded		▓	▓	
60					
80					
90			▓	▓	
40	tare		▓	▓	
60					
80					
90					

DLC: Dynamic load coefficient; LSC: Load sharing coefficient; DLSC: Dynamic load sharing coefficient; DIF: Dynamic impact factor;
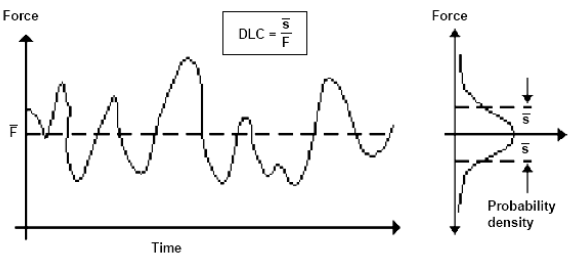PDWF: Peak dynamic wheel force; RSF: Road stress factor.

Appendix 1 – Glossary

Abbreviations and acronyms	Meaning
APT	Air pressure transducer. A device for emitting an electrical signal as a proportional surrogate of input air pressure.
DIF Dynamic Impact Factor	$$DIF = \frac{PDF}{F_{stat(axle)}}$$ Where: PDF = peak instantaneous force; and $F_{stat\,(axle)}$ is the static force (Woodrooffe and LeBlanc, 1987). See also PDWF.
DIVINE	Dynamic Interaction between heavy Vehicles and INfrastructurE.
DLC Dynamic Load Coefficient	Coefficient of variation of dynamic tyre force. It is obtained by calculating the ratio of the root-mean-square (RMS) of the dynamic wheel forces (std dev. of F in diagram below) divided by the static wheel force, *i.e.* the coefficient of variation of the total wheel load: DLC = σ / F_{mean} Where: σ = the standard deviation of wheel force; and F_{mean} = the mean wheel force. A perfect suspension would have a DLC of 0. The range in reality is somewhere between 0 and 0.4 (Mitchell and Gyenes, 1989).

	Figure II.1. Definition of Dynamic Load Coefficient (DLC) (OECD, 1992) *Source:* OECD Road Transport Research, 1992.
DLSC Dynamic load sharing coefficient	The standard deviation of the function of instantaneous dynamic load sharing: DLSi. The instantaneous forces at axle *i* are summed to get F*i* for comparison with the other axle/s in a multi-axle group. DLSC = $\sqrt{\dfrac{\sum (DLS_i - \overline{DLS_i})^2}{k}}$, where: Dynamic load sharing (DLS) at axle *i*, $DLS_i = \dfrac{nF_i}{\sum\limits_{i=1}^{i=n} F_i}$ *n* = number of axles; F*i* = instantaneous wheel-force at axle *i*; and *k* = number of instantaneous values of DLS, *i.e.* number of terms in the series (de Pont, 1997).
HV	Heavy vehicle
LSC Load sharing coefficient	A measure of how well a suspension group equalises the total axle group load averaged over a test. It shows how well the average forces of a multi-axle group are distributed over each tyre and/or wheel in that group. $LSC = \dfrac{F_{mean}(i)}{F_{stat\,(nom)}}$, where: $F_{stat\,(nom)}$ = Nominal static tyre force = $\dfrac{F_{group\,(total)}}{n}$ $F_{group\,(total)}$ = Total axle group force; $F_{mean}(i)$ = the mean force on tyre/wheel *i*; and n = no. of tyres in the group (Potter et al., 1996).
PDSF	Peak dynamic suspension force. The maximum force experienced by any air spring on the test vehicle during a test.
PDWF	Peak dynamic wheel force. The maximum wheel-force experienced by a wheel during dynamic loading as a result of a step input (Fletcher et al., 2002). If applied to axle forces, this measure is the numerator in the equation for dynamic impact factor (DIF).
RFS	"Road-friendly" suspension. HV suspension conforming to certain performance parameters (DOTARS, 2004b).
RSF Road stress factor	An estimation of road damage due to the 4th power of instantaneous wheel force given by: RSF = $(1+6DLC^2 + 3DLC^4)P^4_{stat}$, where DLC is as above and P_{stat} is the static wheel force (Potter *et al.*, 1997).

References

Cebon, D. (Ed.) (1999) *Handbook of vehicle-road interaction*, Swets and Zeitlinger: Netherlands.

Cole, D. J. (1990). *Measurement and analysis of dynamic tyre forces generated by lorries.* Cambrige University Engineering Department: Cambridge, UK.

Davis, L. (2006a). *Dynamic load sharing on air-sprung heavy vehicles: can suspensions be made friendlier by fitting larger air lines?* 29th Australasian Transport Research Forum, 27-29 September: Gold Coast.

Davis, L. (2006b). *Heavy vehicle suspension testing: on-board mass measurement system accuracy and tamper-vulnerability*. Queensland Department of Main Roads: Brisbane.

Davis, L. (2007). *Further developments in dynamic testing of heavy vehicle suspensions*. 30th Australasian Transport Research Forum, 25-27 September, Melbourne.

Davis, L. and Bunker, J. (2008). *Suspension testing of 3 heavy vehicles – methodology and preliminary frequency analysis,* Queensland Department of Main Roads; Queensland University of Technology: Brisbane.

Davis, L. and Sack, R. (2004). *Analysis of heavy vehicle suspension dynamics using an on-board mass measurement system.* 27th Australasian Transport Research Forum, 29 September – 1 October: Adelaide.

De Pont, J. J. (1997). *Assessing heavy vehicle suspensions for road wear*, Transfund New Zealand: Wellington, New Zealand.

De Pont, J. J. (1999). 'Suspensions or whole vehicles? Rating road-friendliness'. *International Journal of Vehicle Design,* 6(1-4), pp. 75-98.

DOTARS (2004a) *Certified road-friendly suspensions*. Department of Transport and Regional Services: Canberra.

DOTARS (2004b) *Certification of road-friendly suspension systems; Road-friendly suspension certification requirements,* Department of Transport and Regional Services: Canberra.

Estill and Associates Pty Ltd (2000) *Operational stability and performance of air suspension on various vehicle configurations*. Department of Transport and Works: Darwin.

Fletcher, C., Prem, H. and Heywood, R. (2002) 'Validation of dynamic load models'. Austroads: Sydney.

Gyenes, L. and Mitchell, C. G. B. (1994). 'The spatial repeatability of dynamic pavement loads caused by heavy goods vehicles'. *Heavy Vehicle Systems: a special series of the International Journal of Vehicle Design,* 1, pp. 156-69.

Hamburg, M. (1983) *Statistical analysis for decision making,* Harcourt, Brace Jovanovich: New York, USA,

Houpis, C. H. and Lamont, G. B. (1985). *Digital control systems theory, hardware, software,* McGraw-Hill: New York, USA.

Kariya, T. and Kurata, H. (2004). *Generalized least squares,* John Wiley and Sons: UK.

Kleyner, A. V. (2005). *Determining optimal reliability targets through analysis of product validation cost and field warranty data*. Department of Mechanical Engineering. University of Maryland, USA.

Lundström, A. A. (2007). *IFRTT October 2007 Newsletter*. International Forum of Road Transport Technology.

Mitchell, C. G. B. and Gyenes, L. (1989). *Dynamic pavement loads measured for a variety of truck suspensions*. 2nd International Symposium on Heavy Vehicles Weights and Dimensions. Roads and Transportation Association of Canada: Kelowna, BC, Canada.

OECD (1998). *Dynamic interaction between vehicles and infrastructure experiment (DIVINE)*. DSTI/DOT/RTR/IR6(98)1/FINAL. Organisation for Economic Co-operation and Development: Paris.

Potter, T. E. C., Cebon, D. and Cole, D. (1997). 'Assessing "road friendliness": A review'. *Journal Automobile Engineering I Mech E,* 211(6). pp. 455-475.

Potter, T. E. C., Cebon, D., Collop, A. C. and Cole, D. J. (1996). 'Road-damaging potential of measured dynamic tyre forces in mixed traffic'. *Proceedings of the Institution of Mechanical Engineers, Part D, Journal of Automobile Engineering,* 210(D3), pp. 215-225.

Potter, T. E. C., Collop, A. C., Cole, D. J. and Cebon, D. (1994). *A34 mat tests: results and analysis*. Cambridge University Engineering Department: Cambridge, UK.

Prem, H., Mai, L. and Brusza, L. (2006). *Tilt testing of two heavy vehicles and related performance issues*. 9th International Symposium on Heavy Vehicle Weights and Dimensions, State College, PA, USA.

Roaduser Systems Pty Ltd (2002) *Stability and on-road performance of multi-combination vehicles with air suspension systems*. National Road Transport Commission: Melbourne.

Statpac Inc (2007) *Statistical significance: One-tailed and two-tailed significance tests*.

Sweatman, P. F. (1983). *A study of dynamic wheel forces in axle group suspensions of heavy vehicles*. Special Report 27. Australian Road Research Board: Vermont South, Vic.

TCA (2007). *Heavy vehicle on-board mass monitoring: Capability review*. Transport Certification Australia Limited: Melbourne.

Willox, N. (2005). *Kenworth's T350 agitator sets new benchmark for construction industry*. <http://www.kenworth.com.au/kenworth/kenworth_newsview.asp?id=57>.

Woodroofe, J. H. F., Leblanc, P. A. and Lepiane, K. R. (1986). *Vehicle weights and dimensions study; volume 11 - effects of suspension variations on the dynamic wheel loads of a heavy articulated highway vehicle*. Canroad Transportation; Roads and Transportation Association of Canada (RTAC): Ottawa, Ontario, Canada.

Woodrooffe, J. H. F. and Leblanc, P. A. (1987). *Heavy vehicle suspension variations affecting road life*. Symposium on Heavy Vehicle Suspension Characteristics. Canberra, Australian Road Research Board: Vermont South, Vic.